ACS APPLIED MATERIALS & INTERFACES

Research Article

www.acsami.org

Sunlight-Induced Self-Healing of a Microcapsule-Type Protective Coating

Young-Kyu Song,[†] Ye-Hyun Jo,[†] Ye-Ji Lim,[†] Sung-Youl Cho,[†] Hwan-Chul Yu,[†] Byung-Cheol Ryu,[‡] Sang-In Lee,[‡] and Chan-Moon Chung*[,†]

[†]Department of Chemistry, Yonsei University, Wonju, Gangwon-do 220-710, Korea

[‡]Korea Conformity Laboratory, 1276 Jisa-dong, Kangseo-ku, Busan, 618-230, Korea

Supporting Information

ABSTRACT: Photopolymerization behavior of a methacryloxypropyl-terminated polydimethylsiloxane (MAT-PDMS) healing agent was investigated in the presence of benzoin isobutyl ether (BIE) photoinitiator by Fourier transform infrared (FT-IR) spectroscopy. MAT-PDMS and BIE were microencapsulated with urea-formaldehyde polymer. The surface and shell morphology of the microcapsules was investigated by scanning electron microscopy (SEM). Mean diameter and size distribution of the microcapsules could be controlled by agitation rate. A coating matrix formulation was prepared by sol−gel reaction of tetraethyl orthosilicate (TEOS) in the presence of a polysiloxane and by subsequent addition of an adhesion promoter. The formulation and microcapsules were mixed to give a self-healing coating formulation, which was then sprayed to surface of cellulose-fiber-reinforced-cement (CRC) board or mortar. Contact angle measurements showed that both the polymerized MAT-PDMS and the prepared coating matrix are hydrophobic, and the coating matrix has good wettability with MAT-PDMS. It was confirmed by optical microscopy and SEM that, when the self-healing coating is damaged, the healing agent is released from ruptured microcapsules and fills the damaged region. The self-healing coating was evaluated as protective coating for mortar, and it was demonstrated by water permeability and chloride ion penetration tests that our system has sunlight-induced self-healing capability. Our self-healing coating is the first example of capsule-type photoinduced self-healing system, and offers the advantages of catalyst-free, environmentally friendly, inexpensive, practical healing.

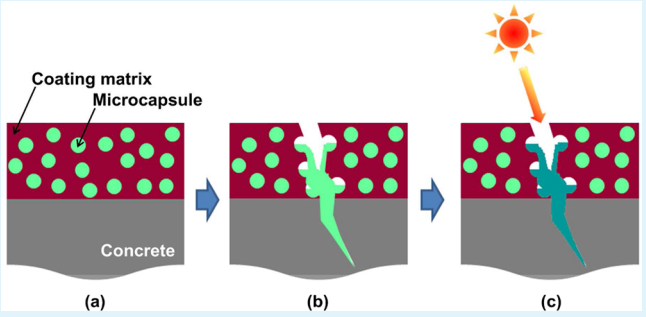

KEYWORDS: *photoinduced self-healing, capsule type, protective coating for concrete, microencapsulation*

INTRODUCTION

Microcrack formation and propagation in materials leads to significant reduction in their mechanical performance and other desired properties.[1−3] Recently, much attention has been paid to self-healing of microcracks to attempt to extend functional lifetime of the materials.[4−10] According to the ways of healing, self-healing polymers and polymer composites can be classified into two categories: (i) intrinsic ones that are able to heal cracks by the materials themselves, and (ii) extrinsic ones in which the healing agent has to be preembedded.[4] In the case of the extrinsic self-healing, matrix resin itself is not a healable one and a healing agent has to be encapsulated and embedded into the materials in advance. As soon as the cracks destroy the microcapsules, the healing agent is released into the crack planes because of the capillary effect and heals the cracks.[4]

A typical extrinsic self-healing system employs a microencapsulated healing agent and a (microencapsulated) catalyst.[11−15] When microcracks propagate through the matrix, the healing agent is released from ruptured microcapsules and polymerizes on contact with the catalyst to repair the damaged region. However, there are limitations of this system, including catalyst availability, cost, environmental toxicity, stability, and materials processing.[16] Recently catalyst-free self-healing systems have been studied to develop less expensive and more practical ways to self-repair polymeric materials. One autonomous, catalyst-free approach is self-healing under natural conditions, for example, in the presence of atmospheric moisture[17,18] and oxygen[19,20] and sunlight.

Photochemical self-healing by UV light or sunlight is a catalyst-free, environmentally friendly, inexpensive, and practical strategy. Photoinduced remending has been accomplished using cinnamates,[21,22] coumarin,[23] anthracene,[24] and chitosan.[25] However, all the previously reported photoinduced self-healing materials are intrinsic healing systems. There has been no report on extrinsic photoinduced self-healing system based on healing-agent-loaded microcapsules, although the microencapsulation of UV-curable silicone oligomers have been reported.[26] Compared to the intrinsic system, the extrinsic one

Received: November 16, 2012
Accepted: February 1, 2013
Published: February 1, 2013

has advantages including the ease of application in most polymer systems and healing of larger damage volume.[5] In this paper, we describe the first example of extrinsic photoinduced self-healing system.

A protective coating is used to protect surface of a material from various deterioration factors. In the case of concrete protective coating, when cracks form and propagate in the coating, water, chloride ion, and carbon dioxide would penetrate through the cracks. This results in the deterioration of concrete, leading to reduction in its serviceability. If the protective coating for concrete has self-healing ability, it would effectively protect the concrete surface from the deterioration. Although several reports of self-healing anticorrosive coatings for metal protection have appear,[17,19,20,27,28] there has been no report on self-healing protective coating for concrete. In this work we have developed a self-healing protective coating system for concrete in which microcracks can be repaired by UV light or sunlight (Figure 1). Healing-agent-loaded micro-

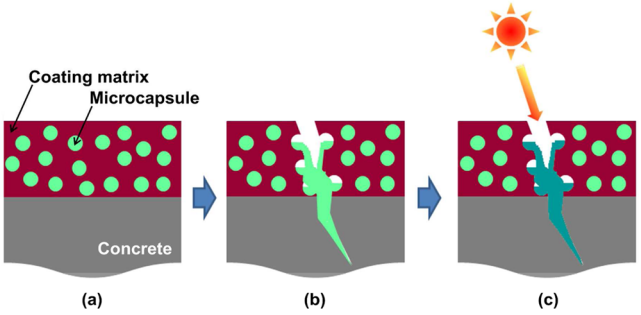

Figure 1. Self-healing concept in this study: (a) self-healing protective coating on concrete; (b) microcapsules are ruptured when cracks are generated and a healing agent is released from ruptured microcapsules and fills the crack plane; (c) cracks are healed by photopolymerization of the healing agent induced by sunlight.

capsules are embedded in a coating matrix to obtain a self-healing protective coating (Figure 1a). Upon damage-induced cracking, the microcapsules are ruptured by the propagating crack fronts, resulting in release of the healing agent into the crack by capillary action and then self-healing is achieved by sunlight (Figure 1b, c).

EXPERIMENTAL SECTION

Materials. Urea, aqueous formaldehyde solution (37 wt %), poly(ethylene-*alt*-maleic anhydride) (EMA), resorcinol, benzoin isobutyl ether (BIE), 1-octanol and tetraethyl orthosilicate (TEOS) were purchased from Sigma-Aldrich. Methacryloxypropyl-terminated polydimethylsiloxane (MAT-PDMS) (molecular weight 380−550 g/mol, viscosity 4−6 cSt) was purchased from Gelest. Ammonium chloride was purchased from Duksan Pharmaceutical. A poly(dimethylsiloxane-*co*-methylphenylsiloxane) fluid (KF-54) was purchased from Shinetsu. An adhesion promoter (Z-6032 Silane) was purchased from Dow Corning. Cellulose-fiber-reinforced-cement (CRC) boards were kindly donated from Samjoongcnc Co. Mortar specimens were prepared according to KSF 2476. All the chemicals and solvents were used without purification.

Instruments. Proton nuclear magnetic resonance (^{1}H NMR) spectra were taken on a Bruker AVANCE II 400 MHz spectrometer in deuteriotetrahydrofuran (THF-d_8) using tetramethylsilane (TMS) as an internal standard. IR spectra were recorded on a Fourier transform infrared (FTIR) spectrophotometer (Spectrum One B, Perkin-Elmer Co.). Photoirradiation was conducted with an exposure system (NEX-SAL, Hantech) equipped with a xenon short arc lamp (light intensity: 22.7 mW/cm^2) in conjunction with a UV cut off filter (>305 nm) (Edmund optics Co.). A mechanical stirrer (NZ-1000, Eyela) was used in microencapsulation. A fluorescence microscope (BX-51, Olympus) was used to take pictures of scribed surface and microcapsules. Microcapsule size was analyzed using a CCD camera (CC-12, Olympus) equipped in the microscope and an image analysis software (analySIS TS, Olympus). Mean diameter and standard deviation were determined from data sets of at least 250 measurements. A scanning electron microscope (SEM) (SU-70, Hitachi) was used to examine surface and shell morphology of the microcapsules and coating surfaces. Microcapsules were mounted on a conductive stage and ruptured with a sharp needle to facilitate observation of the shell morphology. Samples were sputtered with a thin layer (~10 nm) of osmium to reduce charging. A universal testing machine (UTM) (DTU-900MH, Daekyung tech and testing mtg. Co.) was used to generate cracks. Mortar specimens were prepared with a cooling circulation bath (DG-LB, DG & Engineering), a humidity curling chamber (EG-NH, DG & Engineering), a mortar mixer (HJ-1150, Heung Jin Engineering), and a jolting apparatus (SH-APM 100, Shinhan Testing Machine Ind.). Chloride ion penetration test was performed using a RDA-1501 (RADIAN). Static contact angles were determined using a contact angle analyzer (Phoenix 300-Touch, Seo Co).

Measurement of Photopolymerization Conversion. A photocurable mixture was formulated using a mass ratio of MAT-PDMS:BIE of 98:2. The mixture was coated on a KBr disk and photoirradiated with UV light (>305 nm) or sunlight. The exposure of the coating to sunlight was performed in November, 2010. The photopolymerization conversion was measured by FT-IR spectroscopy: the ratios of calculated area of the two absorption bands (1639 cm^{-1} for C═C and 1721 cm^{-1} for C═O as an internal standard) before and after exposure were compared to determine the degree of conversion of the methacrylate C═C bond using the following formula.

$$\text{conversion}\ (\%) = \left(1 - \frac{(\mathrm{C{=}C}_{\text{band area}}/\mathrm{C{=}O}_{\text{band area}})_{\text{after photoirradiation}}}{(\mathrm{C{=}C}_{\text{band area}}/\mathrm{C{=}O}_{\text{band area}})_{\text{before photoirradiation}}}\right) \times 100$$

Microencapsulation. A 2.5 wt % aqueous solution of EMA (3.333 mL) was added in water (13.333 mL), and then urea (0.386 g, 0.006 mol), resorcinol (0.038 g), and ammonium chloride (0.033 g) were added with stirring. pH of the resultant solution was adjusted to 3.5 using a 10% NaOH solution. The resultant mixture was agitated at 1200, 1400, 1600, 1800, or 2000 rpm, and 8 mL of MAT-PDMS containing BIE (mass ratio of MAT-PDMS and BIE is 98:2) was added to obtain an emulsion. After adding a 37% formaldehyde (0.971 g, 0.012 mol) solution, the temperature of the mixture was raised to 55 °C and maintained for 4.5 h. The reaction mixture was cooled to room temperature and microcapsules were isolated by vacuum filtration. The microcapsules were washed with water and THF, and then air-dried. The yields of the microencapsulation ranged from 48 to 93%.

Preparation of Self-Healing Coating. Isopropyl alcohol (69.60 g) and 20.91 g of tetrahydrofuran were put in a 3-neck round-bottom flask in nitrogen atmosphere. To the mixture was added 60.00 g of TEOS and 40.00 g of poly(dimethylsiloxane-*co*-methylphenylsiloxane) and the resultant solution was heated to 80 °C. Distilled water (15.76 g) and 1N HCl (3.65 g) were added into the solution, and the resultant mixture was stirred for 30 min at 80 °C to induce sol−gel reaction. To the resulting mixture was added an adhesion promoter (Z-6032 Silane) to obtain a coating matrix formulation A. The formulation A and microcapsules were mixed with a mass ratio of 7:1 to give a self-healing coating formulation B. The formulation B was sprayed to surface of CRC board or mortar, and then cured for 24 h at room temperature. A control coating was prepared in a similar fashion using the formulation A. All coatings had thickness of 500 ± 50 μm.

Contact Angle Measurements. Static contact angles were determined on surfaces of a polymerized MAT-PDMS or a coating matrix at room temperature (20 °C). Contact angles were measured

within 1 min after applying water or MAT-PDMS droplet to the substrate surface. The tangent to the drop at its intersection with the surface was estimated visually. All reported values are the average of five measurements.

Water Permeability Test. The self-healing coating formulation B or the control coating formulation A was applied to one rectangular side of 40 mm × 40 mm × 130 mm square column mortars. Microcracks were generated in the coated surface of the mortar specimens with a UTM by pressing center part of back side of the coated side to a given extent at a rate of loading of 500 N/min. Cracks were also generated in one rectangular side of plain mortars for comparison. The cracked samples were allowed to heal under sunlight for 4 h. Four side surfaces adjacent to the coated side were covered with epoxy resin, and the cracked surface was brought into contact with water. After 24 h, the increase in mass due to water absorption was determined. For each kind of sample, three specimens were tested and an average of the measured values was taken.

Chloride Ion Penetration Test. The self-healing coating formulation B or the control coating formulation A was applied to one circular cylindrical surface of cylindrical mortars of 100 mm in diameter and 50 mm in thickness. After curing, cylindrical surface of the mortars was covered with epoxy resin. The self-healing and control coatings were scribed with a razor blade, and then allowed to heal under sunlight for 4 h. The chloride ion penetration test was conducted in accordance with ASTM C1202. The specimens were conditioned according to the standard and were subjected to 60-V potential for 6 h. Current values were recorded every 30 min. The total charge that passed through the coated mortar specimens was determined and used to evaluate the chloride ion penetrability of each coating. For each kind of sample, five specimens were used and an average of the measured three values was taken (maximum and minimum values were abandoned).

RESULTS AND DISCUSSION

In this study, a methacryloxypropyl-terminated polydimethylsiloxane (MAT-PDMS) was employed as healing agent. The dimethylsiloxane moiety imparts hydrophobicity and flowability, and the methacrylate moiety, photoreactivity. Because MAT-PDMS gives a hydrophobic solid by photopolymerization (this is described below in detail), the healing agent is considered to be suitable for the protection of substrate surface from water penetration. In addition, MAT-PDMS has low viscosity and a low melting point below −60 °C, so maintains good flowability at very low temperatures and does not need any diluent. One of the important requirements to be a practical healing agent is good flowability at low ambient temperatures. A typical healing agent dicyclopentadiene (DCPD) has a melting point of 33 °C, implying that healing function may not work by freezing of DCPD below the temperature. MAT-PDMS is also considered to be more environmentally friendly than some conventional healing agents that have been used in conjunction with organic diluents.[12,18]

To select a proper photoinitiator, several factors were considered including initiation efficiency of photopolymerization and solubility in MAT-PDMS. We thought that very high initiation efficiency of a photoinitiator would not be desired because polymerization could easily be initiated during preparation and storage of self-healing coating. Benzoin isobutyl ether (BIE) was selected as a photoinitiator because it is not highly efficient, but efficient enough to be used in the self-healing application. In addition, it exists in a liquid state at room temperature and has good solubility in MAT-PDMS. A photocurable mixture was formulated using a mass ratio of MAT-PDMS:BIE of 98:2 and the photopolymerization behavior of MAT-PDMS was investigated by FT-IR spectroscopy. BIE was employed as a radical photoinitiator. The absorption at 1639 cm^{-1} representing the methacrylate C═C stretching vibration gradually decreased with increasing exposure time, indicating the photopolymerization of MAT-PDMS (see the Supporting Information, Figure S1). The ratios of the calculated areas of the two absorption bands (1639 cm^{-1} for C═C and 1721 cm^{-1} for C═O) before and after exposure were compared to determine the degree of conversion of the methacrylate C═C bonds. The absorption band at 1721 cm^{-1} was used as an internal standard for the conversion determination. As shown in Figure 2a, MAT-PDMS showed a

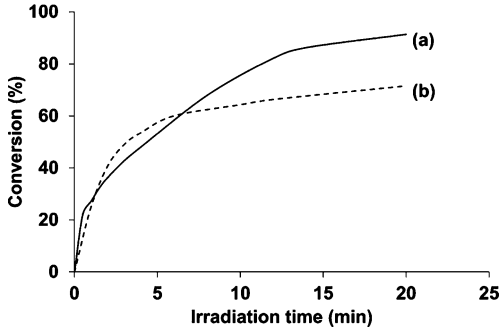

Figure 2. Plot of conversions of MAT-PDMS C═C bond vs irradiation time upon exposure to (a) UV light from xenon lamp and (b) sunlight.

conversion of 91% when irradiated with xenon lamp for 20 min. On the other hand, 72% conversion was achieved upon exposure to sunlight for 20 min (Figure 2b). A hard, transparent solid was obtained by the photo-cross-linking of MAT-PDMS. The measured contact angle of water on a polymerized MAT-PDMS surface was 88°, indicating that the MAT-PDMS polymer is nearly hydrophobic (see the Supporting Information, Figure S2 and Table S1).

We have performed microencapsulation of a mixture of MAT-PDMS and BIE (98:2 by mass) using urea-formaldehyde (UF) polymer as shell material. The UF microcapsules were prepared by in situ polymerization in an oil-in-water emulsion. Agitation rate was varied in the range of 1200−2000 rpm, whereas holding all other factors constant. Yields of the microencapsulation, defined by the ratio of the mass of recovered microcapsules to the total mass of the core and shell constituents, are relatively high: at agitation rates of 1200−1800 rpm, the yields ranged from 82 to 93%. At 2000 rpm, however, the yield decreases to 48%. It was considered that some of the microcapsules were fractured under the high shear condition. During the microencapsulation, it was found by FT-IR spectroscopy that 7% of C═C bonds in MAT-PDMS were consumed. An additional 8% of C═C bonds was consumed during storage of the microcapsules for 22 months in a vial under ambient conditions. It is considered that some of the C═C bonds in MAT-PDMS slowly underwent radical reaction during the microencapsulation and storage period. Although total 15% of C═C bonds reacted after 22 months, the core still had good flowability and photoreactivity, and the amount of the core released from ruptured microcapsules was enough to heal microcracks.

The formation of microcapsules was confirmed by FT-IR and ^1H NMR spectroscopy. As shown in Figure 3a, UF resin shows absorption peaks of N−H and O−H stretching vibration at 3730−3030 cm^{-1}, C═O stretching vibration at 1643 cm^{-1}, and

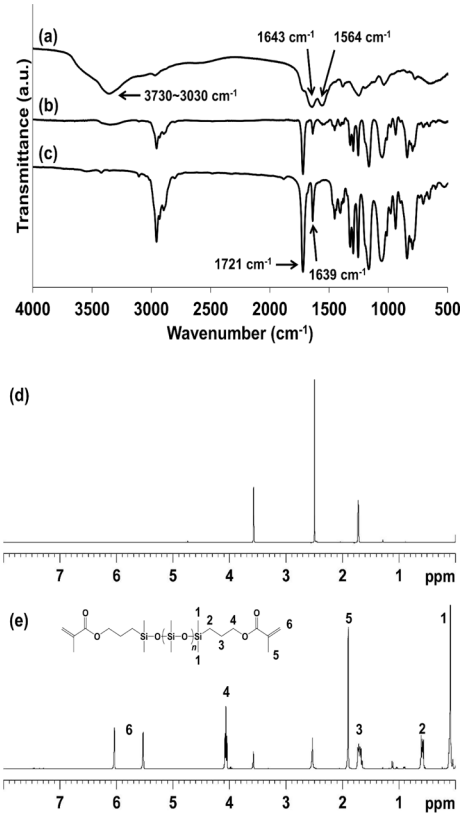

Figure 3. Infrared spectra of (a) UF resin, (b) microcapsules, and (c) MAT-PDMS. ^{1}H NMR spectra of extracts from microcapsules (d) before and (e) after crushing.

C−N stretching vibration at 1564 cm^{-1}. On the other hand, MAT-PDMS shows absorption due to C═O stretching vibration at 1721 cm^{-1} and C═C stretching vibration at 1639 cm^{-1} (Figure 3c). The main absorption peaks of UF resin and MAT-PDMS were observed in the spectrum of the microcapsules (Figure 3b), indicating the successful formation of MAT-PDMS-filled UF microcapsules. To confirm that MAT-PDMS is loaded inside the microcapsules, we performed ^{1}H NMR spectroscopy. First, the microcapsules were washed with THF-d_8, which is a good solvent for MAT-PDMS. The resultant THF-d_8 was found to contain no MAT-PDMS (Figure 3d). In contrast, when the microcapsules were crushed by pressing with a spatula and washed with THF-d_8, it was found that ^{1}H NMR spectrum of the resultant solvent showed peaks of MAT-PDMS (Figure 3e). The results indicate that MAT-PDMS was successfully microencapsulated and the healing agent does not leak out through the capsule wall.

The surface and shell morphology of the microcapsules was investigated by scanning electron microscopy (SEM) (Figure 4a). Spherical microcapsules were obtained at all agitation rates and the outer surface of the capsules is relatively smooth. As the agitation rate increased from 1200 to 2000 rpm, the size distribution narrowed (Figure 4b) and the average diameter of the capsules decreased (Figure 4c, d). The average capsule diameter decreased from 192 to 36 μm with increasing agitation rate from 1200 to 2000 rpm. It is considered that as the agitation rate is increased, a finer emulsion was obtained, leading to the narrower size distribution and smaller average microcapsule diameter.

Our self-healing coating consists of the microcapsules and a coating matrix (Figure 1a), and was prepared as follows. To a solution of TEOS and a polysiloxane in isopropyl alcohol and tetrahydrofuran were added distilled water and an aqueous HCl, and the resultant solution was heated to induce sol−gel reaction. To the resulting mixture was added an adhesion promoter to obtain a coating matrix formulation. The formulation and microcapsules were mixed with a mass ratio of 7:1 to give a self-healing coating formulation. The prepared formulation was sprayed to surface of CRC board or mortar, and the resultant coating was allowed to be cured under ambient conditions for 24 h. It was found that the prepared coating is hydrophobic, based on the measured contact angle of water on the prepared coating (94°) (see the Supporting Information, Figure S2 and Table S1).

For effective crack healing, it is required that the healing agent should readily be released from ruptured microcapsules

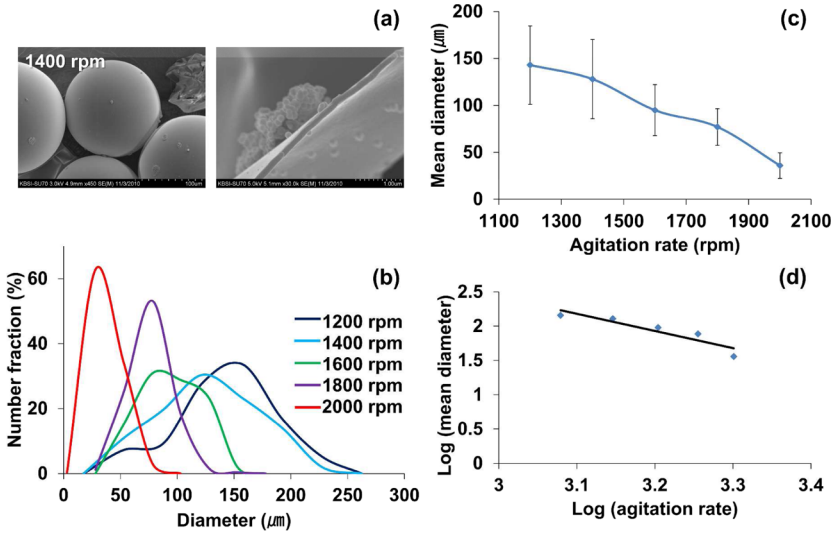

Figure 4. (a) Surface and shell morphology of microcapsules obtained at an agitation rate of 1400 rpm. (b) Microcapsule size distribution at different agitation rates. (c) Average microcapsule diameter as a function of agitation rate. (d) Average microcapsule diameter as a function of agitation rate shown in log−log scale.

dx.doi.org/10.1021/am302728m | ACS Appl. Mater. Interfaces 2013, 5, 1378−1384

and fill the crack plane. Good wettability of the coating matrix with MAT-PDMS is desired for the self-healing mechanism to occur. Contact angle of MAT-PDMS on the coating matrix surface was measured to be 15°, indicating that MAT-PDMS could readily flow into the crack (see the Supporting Information, Figure S2 and Table S1). To evaluate this function of our system, we microencapsulated MAT-PDMS and methyl cinnamate (1 wt % with respect to MAT-PDMS) with UF. Methyl cinnamate was used as a fluorescent indicator. It was confirmed by fluorescence microscopy that, when a coating matrix containing the microcapsules was scribed with a razor blade, the core material was released and filled the scribe region (Figure 5a). In contrast, upon scribing a control coating matrix

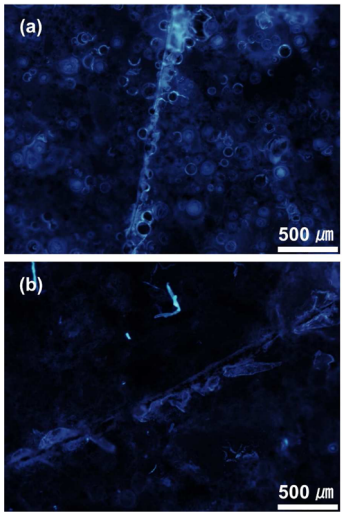

Figure 5. Photographs of scribes formed in (a) a coating with microcapsules containing MAT-PDMS and methyl cinnamate and (b) a control coating without microcapsule. The photographs were obtained using a fluorescence microscope equipped with a CCD camera under 330−385 nm UV light.

without microcapsule, the scribe remained unfilled (Figure 5b). This indicates that upon damage to the self-healing coating, the microcapsules are ruptured and the damaged region is filled with the healing agent.

SEM imaging of the scribe region in the self-healing coating was also performed (Figure 6). The self-healing coating was scribed with a razor blade and exposed to sunlight for 4 h to induce photo-cross-linking. From SEM images of the scribe area in the self-healing coating, it was clearly observed that the MAT-PDMS healing agent filled the scribe and then solidified, indicating effective healing of the scribe (Figure 6a). In contrast, the scribe remained unfilled in the case of the control coating without microcapsule (Figure 6b).

Preliminary evaluation of the self-healing function of our system was conducted through water permeability and chloride ion penetration tests. For the water permeability test, each specimen was prepared by application of the self-healing coating to one rectangular side of a square column mortar, and by generating a microcrack in the coated surface of the mortar by a universal testing machine (UTM). For comparison, microcracks were created in a similar fashion in both plain mortar and control coating mortar specimens. It was observed by optical microscopy that one microcrack of ca.100 μm in width was created in each specimen (Figure 7a, right). Four proximate surfaces of the coated surface were covered with

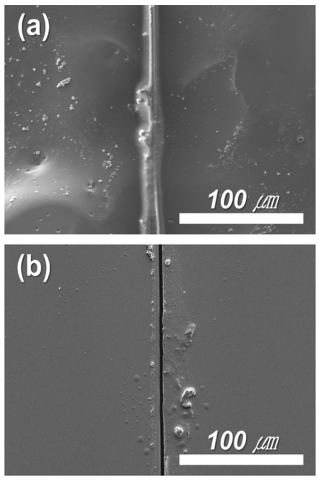

Figure 6. SEM images of scribe region of (a) a self-healing coating after photochemical healing and (b) a control coating without microcapsule.

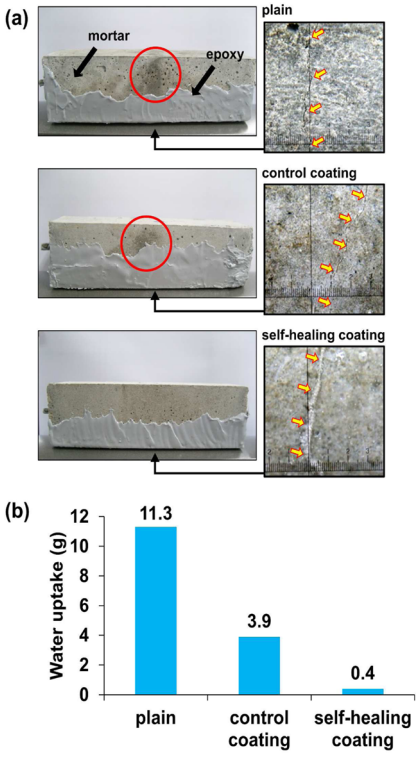

Figure 7. Results of water permeability test for cracked plain or coated mortar specimens. (a) Photographs of side surface (left) and cracked surface (right). The arrows indicate crack position (right). (b) Amount of water uptake upon immersion of the cracked surface in water for 24 h.

epoxy resin to prevent water permeation through the proximate surfaces (Figure 7a, left). The cracked self-healing coating was allowed to heal under sunlight for 4 h. In both cases of the plain mortar and control coating mortar, absorbed water is apparently observed, but the wet part is not seen in the self-healing coating mortar (Figure 7a, left). Figure 7b shows the amount of water uptake of the three kinds of specimens. The cracked plain mortar absorbs the largest amount of water through the crack. In the case of cracked control coating mortar, its water uptake was lower than that of the cracked

plain mortar. When the self-healing coating is cracked, the amount of water uptake corresponds to only 10% of that of the cracked control coating sample. The results suggest that successful self-healing of microcrack was accomplished in our self-healing system, leading to effective prevention of water permeation. It should be noted that the self-healing of "real" cracks formed in the protective coating was accomplished. Most of self-healing coatings have only been evaluated by hand scribing or scratching.[17,19,20,27,28]

Chloride ion penetration test measures the ease with which a protective coating allows the charge to pass through and so gives an indication of the resistance to chloride ion penetration. The total charge that passed through the coated mortar specimens was determined and used to evaluate the chloride ion penetrability of each coating. The test was performed using mortars with the control and self-healing coatings. The coatings were scribed a razor blade, and the scribed self-healing coating was allowed to heal under sunlight for 4 h. While the unscribed control coating shows high resistance to chloride ion penetration (Figure 8a), the scribed control sample reveals

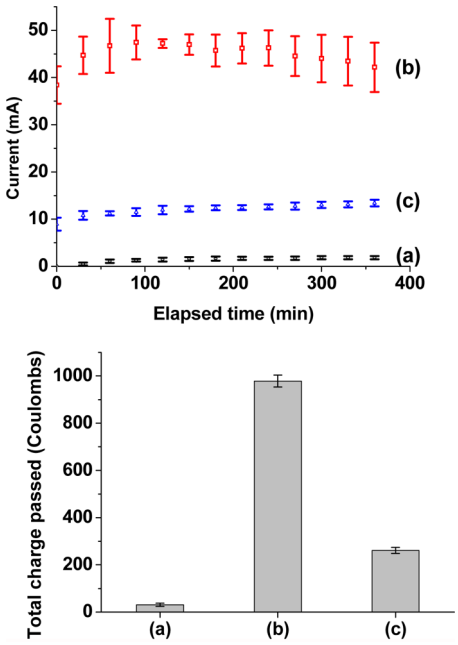

Figure 8. Results of chloride ion penetration test for coated mortar specimens: plots of current vs elapsed time (top) and total charge passed during the 6 h test period (bottom). The tests were performed for specimens with (a) a control coating before scribing, (b) a control coating after scribing, and (c) a self-healing coating that was scribed and then healed under sunlight.

significant increase in chloride ion penetration (Figure 8b). The scribed and healed self-healing coating showed greatly reduced ion penetration property: the total charge value obtained with the self-healing coating corresponds to 27% of that obtained with the scribed control sample. This indicates that the scribe in the self-healing coating was healed by sunlight, largely preventing chloride ion penetration.

CONCLUSIONS

MAT-PDMS healing agent underwent photo-cross-linking reaction by UV light or sunlight in the presence of BIE photoinitiator. A mixture of MAT-PDMS and BIE was microencapsulated with urea-formaldehyde polymer, and the average diameter and size distribution of the resultant microcapsules can be controlled by agitation rate. The microcapsules were embedded in a coating matrix to give the first example of extrinsic photoinduced self-healing system. The combined optical microscopy and SEM results showed that when the self-healing coating is damaged, the healing agent is readily released from ruptured microcapsules, fills damaged area, and solidifies by the photoreaction. The self-healing system was preliminarily evaluated as a protective coating for mortar. It was demonstrated by the water permeability and chloride ion penetration tests that our self-healing system has sunlight-induced healing capability and can effectively protect mortar from deterioration factors such as water and chloride ion. In this work, the evaluation of self-healing material was conducted for the first time as a protective coating for mortar. Our system offers the advantages of catalyst-free, environmentally friendly, inexpensive, practical self-healing.

ASSOCIATED CONTENT

Supporting Information

Infrared spectra of MAT-PDMS before and after exposure and results of contact angle measurements. This material is available free of charge via the Internet at http://pubs.acs.org.

AUTHOR INFORMATION

Corresponding Author

*E-mail: cmchung@yonsei.ac.kr.

Notes

The authors declare no competing financial interest.

ACKNOWLEDGMENTS

This research was supported by Korea Institute of Construction and Transportation Technology Evaluation and Planning grant funded by the Ministry of Land, Transport and Maritime Affairs and by Basic Science Research Program through the National Research Foundation of Korea (NRF) funded by the Ministry of Education, Science and Technology (Grant 2011-0014660).

REFERENCES

(1) Osswald, T.; Menges, G. In *Materials Science of Polymers for Engineers*; Osswald, T., Menges, G., Eds.; Hanser Publishers: Munich, Germany, 2003.
(2) Saucer, J. A.; Hara, M. *Adv. Polym. Sci.* **1990**, *91/92*, 69−118.
(3) Dry, C. *Compos. Struct.* **1996**, *35*, 263−269.
(4) Zhang, M. Q.; Rong, M. Z. *Self-Healing Polymers and Polymer Composites*; Wiley: New York, 2011.
(5) Blaiszik, B. J.; Kramer, S. L. B.; Olugebefola, S. C.; Moore, J. S.; Sottos, N. R.; White, S. R. *Annu. Rev. Mater. Res.* **2010**, *40*, 179−211.
(6) Hager, M. D.; Greil, P.; Leyens, C.; Zwaag, S. v. d.; Schubert, U. S. *Adv. Mater.* **2010**, *22*, 5424−5430.
(7) Murphy, E. B.; Wudl, F. *Prog. Polym. Sci.* **2010**, *35*, 223−251.
(8) Kessler, M. R. *Proc. IMechE Part G: Aerospace Eng.* **2007**, *221*, 479−495.
(9) Wu, D. Y; Meure, S.; Solomon, D. *Prog. Polym. Sci.* **2008**, *33*, 479−522.
(10) Bergman, S. D.; Wudl, F. *J. Mater. Chem.* **2008**, *18*, 41−62.
(11) Xiao, D. S.; Yuan, Y. C.; Rong, M. Z.; Zhang, M. Q. *Polymer* **2009**, *50*, 2967−2975.
(12) Keller, M. W.; White, S. R.; Sottos, N. R. *Adv. Funct. Mater.* **2007**, *17*, 2399−2404.
(13) White, S. R.; Sottos, N. R.; Geubelle, P. H.; Moore, J. S.; Kessler, M. R.; Sriram, S. R.; Brown, E. N.; Viswanathan, S. *Nature* **2001**, *409*, 794−797.
(14) Coope, T. S.; Mayer, U. F. J.; Wass, D. F.; Trask, R. S.; Bond, I. P. *Adv. Funct. Mater.* **2011**, *21*, 4624−4631.

(15) Rule, J. D.; Brown, E. N.; Sottos, N. R.; White, S. R.; Moore, J. S. *Adv. Mater.* **2005**, *17*, 205−208.
(16) Caruso, M. M; Delafuente, D. A.; Ho, V.; Sottos, N. R.; Moore, J. S.; White, S. R. *Macromolecules* **2007**, *40*, 8830−8832.
(17) Huang, M.; Yang, J. *J. Mater. Chem.* **2011**, *21*, 11123−11130.
(18) Yang, J.; Keller, M. W.; Moore, J. S.; White, S. R.; Sottos, N. R. *Macromolecules* **2008**, *41*, 9650−9655.
(19) Suryanarayana, C.; Rao, K. C.; Kumar, D. *Prog. Org. Coat.* **2008**, *63*, 72−78.
(20) Jadhav, R. S.; Hundiwale, D. G.; Mahulikar, P. P. *J. Appl. Polym. Sci.* **2011**, *119*, 2911−2916.
(21) Chung, C. M; Roh, Y. S.; Cho, S. Y.; Kim, J. G. *Chem. Mater.* **2004**, *16*, 3982−3984.
(22) Cho, S. Y.; Kim, J. G.; Chung, C. M. *J. Nanosci. Nanotechnol.* **2010**, *10*, 6972−6976.
(23) Ling, J.; Rong, M. Z.; Zhang, M. Q. *J. Mater. Chem.* **2011**, *21*, 18373−18380.
(24) Froimowicz, P.; Frey, H.; Landfester, K. *Macromol. Rapid Commun.* **2011**, *32*, 468−473.
(25) Ghosh, B.; Urban, M. W. *Science* **2009**, *323*, 1458−1460.
(26) Xing, R.-Y.; Zhang, Q.-Y.; Sun, J.-L. *Polym. Polym. Comp.* **2012**, *20*, 77−82.
(27) Samadzadeh, M.; Boura, S. H.; Peikari, M.; Kasiriha, S. M.; Ashrafi, A. *Prog. Org. Coat.* **2010**, *68*, 159−164.
(28) Cho, S. H.; White, S. R.; Braun, P. V. *Adv. Mater.* **2009**, *21*, 645−649.